UC Irvine

UC Irvine Previously Published Works

Title

Alzheimer-related altered white matter microstructural integrity in Down syndrome: A model for sporadic AD?

Permalink

https://escholarship.org/uc/item/5rs407xs

Journal

Alzheimer's & dementia (Amsterdam, Netherlands), 12(1)

ISSN

2352-8729

Authors

Rosas, H Diana
Hsu, Eugene
Mercaldo, Nathaniel D
et al.

Publication Date

2020

DOI

10.1002/dad2.12040

Peer reviewed

eScholarship.org Powered by the California Digital Library
University of California

Received: 27 December 2019 | Revised: 14 February 2020 | Accepted: 19 February 2020 | Published online: 27 July 2020

DOI: 10.1002/dad2.12040

Alzheimer's & Dementia
Diagnosis, Assessment & Disease Monitoring

DIAGNOSTIC ASSESSMENT & PROGNOSIS

Alzheimer-related altered white matter microstructural integrity in Down syndrome: A model for sporadic AD?

H. Diana Rosas[1,2] | **Eugene Hsu**[1,2] | **Nathaniel D. Mercaldo**[1] | **Florence Lai**[1] | **Margaret Pulsifer**[1] | **David Keator**[3] | **Adam M. Brickman**[4,5] | **Julie Price**[2] | **Michael Yassa**[6] | **Christy Hom**[3] | **Sharon J. Krinsky-McHale**[7] | **Wayne Silverman**[8,9] | **Ira Lott**[9] | **Nicole Schupf**[4,5,10]

[1]Department of Neurology, Massachusetts General Hospital, Harvard Medical School, Boston, Massachusetts, USA

[2]Department of Radiology, Athinoula Martinos Center, Massachusetts General Hospital, Harvard Medical School, Charlestown, Massachusetts, USA

[3]Department of Psychiatry and Human Behavior, University of California, Irvine, California, USA

[4]G. H. Sergievsky Center and Taub Institute for Research on Alzheimer's Disease and the Aging Brain, College of Physicians and Surgeons, Columbia University, New York, New York, USA

[5]Department of Neurology, College of Physicians and Surgeons, Columbia University, New York, New York, USA

[6]Department of Neurobiology and Behavior, University of California, California, USA, Irvine

[7]New York Institute for Basic Research in Developmental Disabilities, New York, New York, USA

[8]Kennedy Krieger Institute, Johns Hopkins University School of Medicine, Baltimore, Maryland, USA

[9]Department of Pediatrics, Irvine Medical Center, University of California, Irvine, California, USA

[10]Department of Epidemiology, Mailman School of Public Health, Columbia University, New York, New York, USA

Correspondence
H. Diana Rosas, 149 13th Street, Room 10126, Charlestown, MA 02129, USA.
E-mail: rosas@helix.mgh.harvard.edu

Funding information
National Institutes of Health, Grant/Award Number: NIA 1U01AG051412

Eugene Hsu, Nathaniel D. Mercaldo, Florence Lai, and Margaret Pulsifer have contributed equally to this manuscript.

Funding information:
This work was supported by National Institutes of Health NIA 1U01AG051412.

Abstract

Introduction: Virtually all adults with Down syndrome (DS) develop Alzheimer's disease (AD)-associated neuropathology by the age of 40, with risk for dementia increasing from the early 50s. White matter (WM) pathology has been reported in sporadic AD, including early demyelination, microglial activation, loss of oligodendrocytes and reactive astrocytes but has not been extensively studied in the at-risk DS population.

Methods: Fifty-six adults with DS (35 cognitively stable adults, 11 with mild cognitive impairment, 10 with dementia) underwent diffusion-weighted magnetic resonance imaging (MRI), amyloid imaging, and had assessments of cognition and functional abilities using tasks appropriate for persons with intellectual disability.

Results: Early changes in late-myelinating and relative sparing of early-myelinating pathways, consistent with the retrogenesis model proposed for sporadic AD, were associated with AD-related cognitive deficits and with regional amyloid deposition.

Discussion: Our findings suggest that quantification of WM changes in DS could provide a promising and clinically relevant biomarker for AD clinical onset and progression.

KEYWORDS

Alzheimer's disease, Down syndrome, white matter integrity

 © 2020 the Alzheimer's Association

1 | INTRODUCTION

Down syndrome (DS) is the most common genetic cause of intellectual disability (ID).[1] It is associated with overexpression of more than 300 genes located on the trisomic chromosome 21[2] that results in the syndrome. Improvements in quality of care for individuals with DS, and quality of life more broadly, have resulted in a longer lifespan. However, virtually all adults with DS develop neuropathology consistent with a diagnosis of Alzheimer's disease (AD) by the age of 40 and most will develop dementia by age 60 to 65.[3] This increased risk has been attributed largely to the triplication of amyloid precursor protein (APP) on chromosome 21,[4] which results in the deposition of extracellular amyloid beta (Aß) in neuritic plaques leading to neurofibrillary pathology and which can be seen as amyloid-positivity on positron emission tomography (PET) scans.[5-7] Aß deposits and APP accumulation have been observed in the white matter (WM) of the frontal cortex in DS. Aß deposits have been shown to be cytotoxic to oligodendrocytes. WM changes specifically associated with AD in individuals with DS have been reported in *post mortem* studies, including evidence of demyelination, microglial activation, loss of oligodendrocytes, and reactive astrocytes.[1,8-10] Studies using diffusion weighted imaging (DWI) have reported altered structural connectivity in cognitively stable (CS) adults with DS;[11,12] it is possible that regional changes in WM integrity confer a particular susceptibility of individuals with DS to develop dementia.

We sought to examine differences in WM integrity among adults with DS participating in a multi-site research consortium established to identify biomarkers associated with AD in older adults with DS. As part of this study, participants underwent a comprehensive set of neuropsychological assessments as well as neuroimaging. The cohort that completed diffusion weighted imaging included a total of 56 individuals with DS, 35 who were cognitively stable (CS) individuals, 11 with a consensus diagnosis of mild cognitive impairment (MCI-DS), and 10 meeting a consensus diagnosis of dementia (DEM).

We compared measures of WM integrity across the three diagnostic groups. We used a diffusion tractography method for the automated reconstruction of 18 major cerebral white matter fiber bundles entitled tracts constrained by underlying anatomy (TRACULA)[13] to evaluate distinct diffusion measures. These included: (1) fractional anisotropy (FA), a scalar measure that provides an indication of the directional coherence of water and is considered highly sensitive to WM features including myelination, axonal degeneration, axonal packaging, and cytoskeletal features;[14,15] (2) mean diffusivity (MD), which describes the rotationally invariant magnitude of water diffusion within brain tissue and can be affected by any disease process that affects the barriers that restrict the motion of water;[16] (3) radial (perpendicular) diffusivity (RD), which has been associated with WM demyelination or dysmyelination, as well as changes in axonal diameter or density; and (4) axial (parallel) diffusivity (AxD), believed to be sensitive to axonal degeneration.[17] Previous studies have suggested that in sporadic AD, WM alterations are thought to initially involve medial temporal limbic association tracts and then spread to involve temporal and white matter with disease progression.[18-20] We were therefore particularly interested in limbic and cortico-cortical projection fibers.

Several recent studies in sporadic AD have suggested decreased regional WM integrity correlated with cognitive dysfunction.[11,21] Thus, we evaluated the relationship between neuropsychological tests assessing memory with limbic WM tracts, taking into account severity

HIGHLIGHTS

- Virtually all adults with Down syndrome (DS) develop Alzheimer's disease (AD)-associated neuropathology by the age of 40.
- Early changes in white matter (WM) microstructure in late-myelinating pathways occur.
- Later WM changes occur in early-myelinating pathways, consistent with retrogenesis model.
- WM changes are associated with neuropsychological test performance, amyloid positron emission tomography uptake.
- Regional WM changes are predictive of mild cognitive impairment in DS.
- WM changes may provide an important biomarker for AD clinical onset and progression.

RESEARCH IN CONTEXT

1. Systematic review: The authors reviewed the literature using traditional (eg, PubMed) sources and meeting abstracts and presentations. White matter (WM) microstructural abnormalities have not as yet been widely studied as contributors to aging-related cognitive decline in adults with Down syndrome (DS). However, several publications discuss the importance of WM changes in sporadic Alzheimer's disease (AD) and we therefore extended this research to the high-risk population with DS.
2. Interpretation: Our findings of WM microstructural abnormalities in the development of AD in adults with DS in a pattern consistent with sporadic AD suggest parallels in disease progression. Therefore, longitudinal studies of adults with DS, with their exceptionally high risk for developing AD, may provide valuable insights into AD progression more broadly.
3. Future directions: This article proposes a novel framework for the generation of new hypotheses related to the role of WM microstructural abnormalities in cognitive decline in AD in adults with and without DS.

of intellectual disability (and unrelated to AD clinical progression). Finally, we evaluated the relationship between altered WM integrity of tracts projecting to cortical areas involved in memory function and regional amyloid deposition.

2 | MATERIALS AND METHODS

2.1 | Participants

Participants were recruited through the Alzheimer's Disease in Down Syndrome (ADDS) component of the Alzheimer's Biomarker Consortium-Down Syndrome (ABC-DS) established to identify biomarkers associated with AD in older adults with DS. Massachusetts General Hospital; University of California, Irvine; and Columbia University/New York State Institute for Basic Research in Developmental Disabilities served as enrolling sites. Inclusion criteria for the study were: (1) ≥40 years of age at baseline, (2) estimated premorbid IQ ≥ 30, (3) Trisomy 21 as confirmed by genetic testing, and (4) English speaker. Premorbid level of functioning was determined from previous testing or caregiver report. The work was done in accordance with the Declaration of Helsinski. Institutional Review Board approval was obtained at participating institutions; informed consent as well as participant assent were obtained in all cases.

2.2 | Assessments

As part of the overall study design, participants received a comprehensive assessment that included: (1) detailed review of medical records; (2) informant interviews focused on functional and vocational abilities, neuropsychiatric status, health status, and life events that might cause substantial stress; and (3) direct one-on-one tests covering the breadth of cognitive abilities expected to be affected by AD. Finally, each participant was examined by a neurologist familiar with this population. Assessments were reviewed to determine the clinical status of each participant at a Consensus Review Conference,[22] which included site senior staff members and research assistants who had direct contact with the participants under consideration.

Clinical status was classified into the following, generally consistent with recommendations of the AAMR-IASSID Working Group for the Establishment of Criteria for the Diagnosis of Dementia in Individuals with Developmental Disability:[23,24] (1) CS, indicating with reasonable certainty that clinically significant declines were absent; (2) MCI-DS, indicating that there were indicators of mild cognitive and/or functional decline beyond what would be expected with aging, per se, but of insufficient severity to suggest frank dementia; (3) definite dementia, indicating with high confidence that dementia was present based upon substantial decline over time; (4) possible dementia, indicating that some signs and symptoms of dementia were present but declines over time were not judged to be totally convincing. For the present analyses, participants from the two dementia classifications were combined into a single "Dementia (DEM)" group.

Fifty-six individuals completed DWI, PET amyloid imaging, and a comprehensive neuropsychological assessment. The current analyses examined the relationship between DWI and baseline memory functioning as well as consensus rating because changes in memory are an early symptom of sporadic AD. Several explicit memory measures were included in the analyses. The Cued Recall Test (CRT)[25] was adapted from a 12-item list learning task assessing verbal learning and memory; the total recall scores includes the summation of the free recall score and the cued recall score. The Rivermead Behavioral Memory Test[26] (Children's version) Picture Recognition (PR) subtest requires the participant to initially identify 10 line drawings of common objects and then later recognize the original 10 drawings as compared to 10 distractors. The Test of Severe impairment (TSI) is a valid and reliable test of cognitive function in individuals with cognitive impairment.[27] The Down Syndrome Mental State Exam (DSMSE)[28] subtest assesses visual immediate and delayed visual memory of nine common objects. For this study, a Total Memory Score (TMS; DSMSE Memory subtest + Shoe Box Memory Test[24]) was calculated and used for analyses.

3 | EXPERIMENTAL DESIGN

3.1 | MRI/PET acquisition

Magnetic resonance imaging (MRI): Imaging data were collected at Massachusetts General Hospital (MGH) and Columbia using a Siemens Prisma 3-Tesla scanner equipped with a 32-channel head coil. A T1-weighted Multi-Echo MPRAGE was collected with the following parameters: repetition time (TR): 2510.00 ms, echo time (TE): 1.69 ms. Flip angle: 7.00°, voxel size 1.0 isotropic, image matrix size 256 × 256 × 176, field of view (FOV) 256 × 256 mm. DWI included the following parameters: TR/TE/Flip angle 8900 ms/80 ms/90°, 30 non-colinear directions, b = 900 s/mm^2, 110 × 110 × 72 image matrix. Imaging data was collected at University of California Irvine (UCI) using a Philips 3-Tesla scanner equipped with a 32-channel head coil using a harmonized protocol. A T1 weighted Multi-Echo MPRAGE was collected using the following parameters TR/TE/Flip angle 7.8 ms/3.6 ms/7°, voxel sizes 1.0 isotropic, image matrix size 256 × 256 × 176, FOV 256 × 256 mm. DWI imaging included the following parameters: TR/TE/Flip angle 10,900 ms/97 ms/90°, 60 non-colinear directions, b = 70, 900 s/mm^2, 128 × 128 × 76 image matrix.

Amyloid PET: 18F-AV-45 (florbetapir) PET scans were acquired at UCI and MGH. Participants from UCI were scanned on a high resolution research tomograph (HRRT; orientation = axial, voxel size = 1.2 mm^3, matrix size = 256 × 256 × 207, reconstruction = OP-OSEM3D); Columbia University on a Siemens Biograph 64 mCT (axial, voxel size = 1.0 × 1.0 × 2.0 mm, matrix size = 400 × 400 × 436, reconstruction = OSEM3D+TOF 4i21s); at MGH on a Siemens Biograph mMR (axial, voxel size = 2.1 × 2.1 × 2.0 mm, matrix size = 344 × 344 × 127, reconstruction = OP-OSEM 3i21s). Protocols consisted of 4 × 5 minute frames collected 50 to 70 minutes after injection of the ligand. PET

reconstructions were performed with attenuation and scatter correction as implemented on each platform.

3.1.1 | Automated anatomical segmentation

Automated cortical parcellations and subcortical segmentation were obtained through processing and reconstruction of the anatomical data using FreeSurfer (https://surfer.nmr.mgh.harvard.edu, software package version 6.0), as described previously.[29]

3.2 | Diffusion analyses: TRACULA

Diffusion-weighted images were processed in a blinded fashion, using TRACULA, available as part of FreeSurfer.[13,30] To reconstruct known WM bundles, TRACULA uses prior information of the anatomy from a set of training participants for which the tracts of interest were labeled manually. This prior information provides the probability each tract travels through or next to each of the cortical and subcortical segmentation labels from FreeSurfer. The output of TRACULA is a probabilistic distribution for each of the 18 tracts, derived in the individual's own anatomical space.[30]

Data were preprocessed to correct for simple head motion and eddy currents by aligning the diffusion weighted images to an average of the first $b = 0$ image of the diffusion series, using a standard linear registration tool available as part of FSL (http:www.fmrib.ox.ac.uk/fsl). FreeSurfer's boundary-based registration method[31] was used for the affine intra-subject alignment between the diffusion-weighted and anatomical images, and to an MNI152 template. Tensors were fit to the DWI data using a standard least squares tensor estimation method and FA, AxD, and RD volumes were computed from the tensors. Note that tensors were used to compute these measures. TRACULA uses FSL's bedpost X tool to fit the ball-and-stick model of diffusion. This comprises two anisotropic compartments per voxel, which model distinct axon populations, and one isotropic compartment per voxel. TRACULA then uses the individual participant's local diffusion orientations, from the anisotropic compartments of the ball-and-stick model, as well as the participant's cortical and subcortical segmentation labels combined with prior information on each tract's position relative to these labels (based on the training set) to estimate the probability distributions of each tract. This allows the reconstruction of volumetric distributions of major WM pathways and the extraction of tensor-based measures for each of the reconstructed pathways. The major WM pathways include the forceps major (FMajor), forceps minor (FMinor), L/R corticospinal tract (CST), L/R inferior longitudinal fasciculus (ILF), L/R uncinate fasciculus (UNC), L/R anterior thalamic radiation (ATR), L/R cingulum-cingulate gyrus bundle (CCG), L/R cingulum-angular bundle (CAB), L/R superior longitudinal fasciculus-parietal bundle (SLFp), L/R superior longitudinal fasciculus-temporal bundle (SLFt), for a total of 18 tracts. All raw and processed images were visually inspected to ensure that they met quality standards for analysis.

3.3 | Amyloid analyses

Reconstructed PET scan frames were realigned and averaged prior to analysis. The resulting images were co-registered with their respective T1-weighted structural MRIs. For region of interest (ROI) analyses and standardized uptake value ratio (SUVR) scaling, volumetric segmentations of the MRI scans were computed with FreeSurfer (FS6 version 6.0)[32] and visually checked for accuracy and corrected when necessary. PET counts were converted to SUVR units using the cerebellum-cortex reference region prior to computing ROI averages. MRI-derived voxel-weighted SUVR averages for each ROI were extracted in native space using individualized FS6 atlas segmentations.[33] We focused on the following ROIs and possible associations with specific tracts: the entorhinal cortex, parietal lobe, and precuneus, which carry projections from the cingulum; superior frontal, middle frontal, and entorhinal and the FMinor; precuneus, parietal, lingual and lateral occipital, and the FMajor.

3.4 | Statistical analyses

Categorical variables were summarized as percentages and as frequencies. Differences in categorical variables were assessed using either the Chi-square test or Fisher's exact test, as appropriate. Continuous variables were summarized as the mean (standard deviation). Differences in continuous variables were assessed using an analysis of variance (ANOVA). We summarized the distribution of FA values for select tracts using violin plots, with superimposed boxplots by disease diagnosis.

A series of linear regression models was constructed in which the diffusion value was regressed onto disease diagnosis and age. F- and Wald tests were performed to assess the overall effect of diagnosis, as well as a pairwise diagnosis comparison between CS and MCI-DS. A trend test was performed to quantify monotonic associations between each diffusion measure and diagnosis using a partial Spearman correlation that accounted for age. Diagnosis-specific point estimates, and 95% confidence intervals (CI), were computed for each tract. False discovery rate (FDR) adjusted *P*-values were computed to account for multiple comparisons across diffusion measures.[34] Both unadjusted *P*-values are provided, along with FDR-adjusted *P*-values (labeled *q*). Partial Spearman correlation values, accounting for age, were computed between FA diffusion measures and predetermined neuropsychological instruments and with predefined ROIs of amyloid SUVR.

A series of logistic regression models was constructed to quantify the ability of each diffusion measure to discriminate between groups (CS vs MCI-DS and CS vs DEM), using the estimation of optimism-adjusted area under the receiver operator characteristic curves, along with bootstrapped 95% confidence intervals. Similarly, a penalized logistic regression (via relaxed least absolute shrinkage and selection operator [LASSO] and 10-fold cross-validation) was used to estimate similar quantities using all FA measures simultaneously. All analyses were performed using R 3.5.2.[35]

TABLE 1 Demographics and neurologic assessments by diagnostic group

	Cognitively stable N = 35	MCI-DS N = 11	Dementia N = 10	*P-value*
Age	48.5 (6.1), 35	51.5 (5.2), 11	54.3 (7.7), 10	0.034
Sex, % (N)				0.447*
Male	63 (22)	82 (9)	60 (6)	
Female	37 (13)	18 (2	40 (4)	
Intellectual disability, % (N)				0.163*
Mild	60 (18)	22 (2)	62 (5)	
Moderate	37 (11)	56 (5)	38 (3)	
Severe	3 (1)	22 (2)	0 (0)	
Test for severe Impairment score	21.37 (4.03), 30	20.44 (2.55), 9	21.14 (2.48), 7	0.799
Total memory score	13.42 (5.10), 31	11.44 (4.00), 9	5.12 (2.70), 8	<0.001
Cued recall total score	28.52 (9.57), 27	20.78 (10.45), 9	15.20 (12.03), 5	0.014
Rivermead score	4.96 (3.93), 27	3.0 (4.17), 8	2. 62(3.07), 8	0.215

Notes: Continuous variables are summarized using mean and standard deviation, number of non-missing responses and categorical variables are summarized as percentages (frequency). Group comparisons were performed using either the chi-square test or Fisher's exact test (as denoted by the asterisk by the *P*-value) for categorical variables and an analysis of variance for continuous variables.
Abbreviation: MCI-DS, mild cognitive impairment-Down syndrome

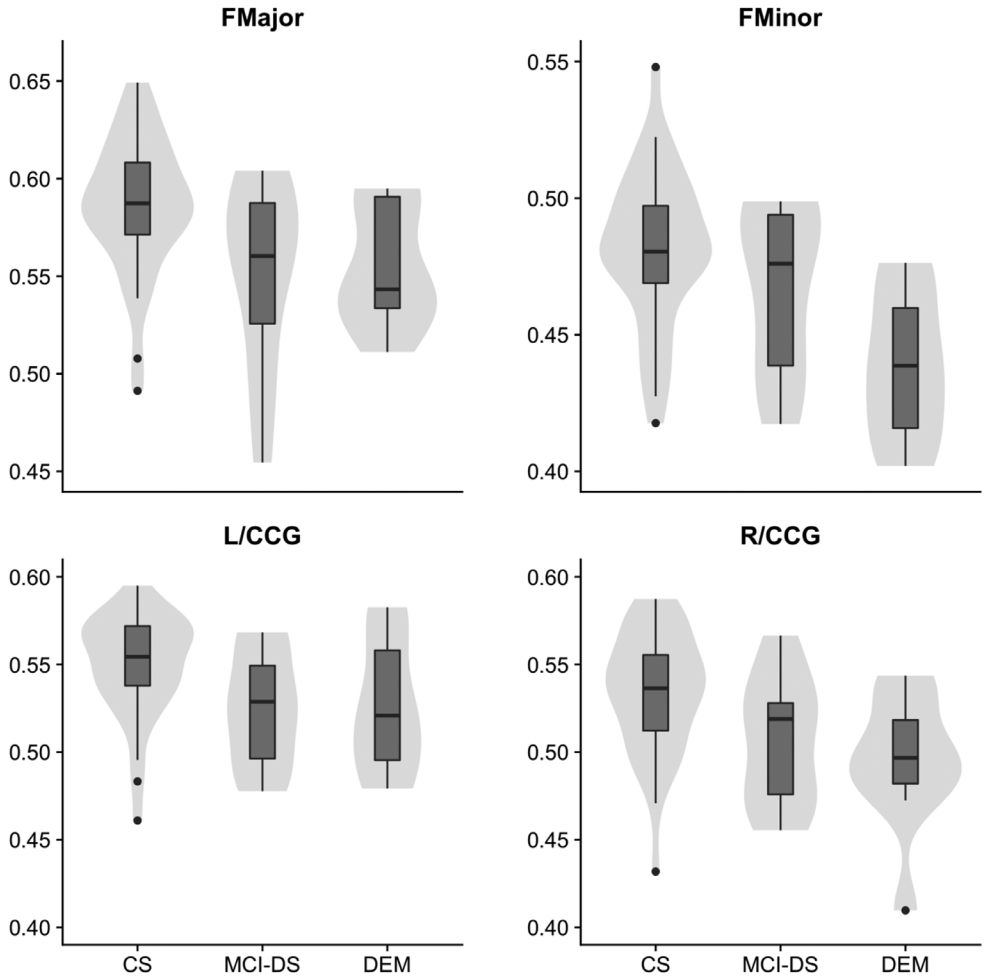

FIGURE 1 Violin and box plots describing the distribution of fractional anisotropy by diagnostic group. Fractional anisotropy values among mild cognitive impairment-Down syndrome subjects were significantly lower in the forceps major, forceps minor, and left/right cingulum-cingulate gyrus bundle compared to cognitively stable subjects

TABLE 2 Fractional anisotropy summaries by diagnostic group and tract

	Cognitively stable (CS) Estimate(95% CI)	MCI-DS Estimate(95% CI)	Dementia Estimate(95% CI)	p_{trend} (q_{trend})	MCI-DS – CS Difference(95%CI)	MCI-CS; *P-value* (*q*)
FMajor	0.58 [0.57, 0.60]	0.55 [0.52, 0.57]	0.56 [0.54, 0.59]	0.046 (0.132)	−0.04 [−0.06,−0.01]	0.005 (0.044)
FMinor	0.48 [0.47, 0.49]	0.46 [0.43, 0.48]	0.45 [0.42, 0.47]	0.029 (0.099)	−0.02 [−0.04, 0.00]	0.086 (0.218)
L ATR	0.41 [0.40, 0.42]	0.41 [0.39, 0.43]	0.42 [0.41, 0.44]	0.230 (0.430)	0.00 [−0.02, 0.02]	0.941 (0.973)
L CAB	0.36 [0.34, 0.38]	0.35 [0.31, 0.39]	0.32 [0.28, 0.37]	0.034 (0.111)	−0.01 [−0.05, 0.03]	0.632 (0.785)
L CCG	0.55 [0.54, 0.56]	0.52 [0.50, 0.55]	0.53 [0.50, 0.55]	0.038 (0.117)	−0.03 [−0.05, 0.00]	0.030 (0.102)
L CST	0.55 [0.53, 0.56]	0.54 [0.52, 0.57]	0.54 [0.51, 0.56]	0.436 (0.647)	0.00 [−0.03, 0.02]	0.731 (0.868)
L ILF	0.45 [0.44, 0.46]	0.44 [0.42, 0.46]	0.43 [0.40, 0.45]	0.011 (0.061)	−0.01 [−0.04, 0.01]	0.217 (0.422)
L Slfp	0.42 [0.41, 0.43]	0.42 [0.40, 0.44]	0.40 [0.38, 0.42]	0.104 (0.259)	−0.01 [−0.03, 0.01]	0.556 (0.722)
L Slft	0.45 [0.44, 0.46]	0.45 [0.43, 0.47]	0.43 [0.41, 0.45]	0.141 (0.323)	0.00 [−0.02, 0.02]	0.732 (0.868)
L Unc	0.38 [0.37, 0.40]	0.38 [0.35, 0.40]	0.36 [0.34, 0.39]	0.187 (0.395)	−0.01 [−0.03, 0.02]	0.527 (0.720)
R ATR	0.41 [0.40, 0.42]	0.40 [0.38, 0.42]	0.41 [0.39, 0.43]	0.748 (0.871)	−0.01 [−0.02, 0.01]	0.363 (0.579)
R CAB	0.37 [0.36, 0.38]	0.35 [0.33, 0.38]	0.33 [0.30, 0.36]	0.007 (0.048)	−0.02 [−0.04, 0.01]	0.201 (0.402)
R CCG	0.53 [0.52, 0.55]	0.51[0.48, 0.53]	0.50 [0.47, 0.53]	0.004 (0.035)	−0.03 [−0.05, 0.00]	0.047 (0.134)
R CST	0.52 [0.51, 0.53]	0.53 [0.51, 0.55]	0.51 [0.49, 0.54]	0.408 (0.618)	0.00 [−0.02, 0.03]	0.750 (0.871)
R ILF	0.46 [0.45, 0.47]	0.44 [0.42, 0.47]	0.42 [0.40, 0.44]	0.003 (0.031)	−0.01 [−0.04, 0.01]	0.181 (0.388)
R Slfp	0.42 [0.41, 0.43]	0.42 [0.40, 0.44]	0.40 [0.38, 0.42]	0.313 (0.524)	0.00 [−0.02, 0.02]	0.786 (0.887)
R Slft	0.43 [0.42, 0.44]	0.43 [0.41, 0.46]	0.43 [0.40, 0.45]	0.461 (0.668)	0.00 [−0.02, 0.02]	0.912 (0.959)
R UNC	0.39 [0.38, 0.40]	0.38 [0.36, 0.41]	0.36 [0.34, 0.38]	0.019 (0.082)	−0.01 [−0.03, 0.01]	0.514 (0.718)

Notes: Main effect estimates (CS, MCI-DS, and Dementia subjects) with corresponding 95% confidence intervals; comparison columns (MCI-DS vs CS) correspond to expected FA changes after adjusting for age. Monotonic trends were assessed using the partial Spearman correlation that accounted for age. Unadjusted *P*-values are presented (*P*) as well as FDR-adjusted *p*-values (*q*) that account for multiple testing of fractional anisotropy (FA), axial diffusivity (AxD), mean diffusivity (MD), and radial diffusivity (RD) across all tracts. Tracts include: forceps major (FMajor), forceps minor (FMinor), L/R corticospinal tract (CST), L/R inferior longitudinal fasciculus (ILF), L/R uncinate fasciculus (UNC), L/R anterior thalamic radiation (ATR), L/R cingulum-cingulate gyrus bundle (CCG), L/R cingulum-angular bundle (CAB), L/R superior longitudinal fasciculus-parietal bundle (SLFp), L/R superior longitudinal fasciculus-temporal bundle (SLFt).
Abbreviation: MCI-DS, mild cognitive impairment-Down syndrome; FDR, false discovery rate

4 | RESULTS

4.1 | Demographics

Demographics and neuropsychological test scores are shown in Table 1. On average, patients diagnosed with dementia tended to be older than other diagnostic groups ($P = 0.034$). A majority of the sample (approximately 60%) of the sample was previously identified with mild intellectual disability. We were unable to detect differences in baseline level of intellectual disability by diagnostic groups ($P = 0.799$).

4.2 | Diagnostic group comparisons of diffusion measures

The distributions of diffusion values by diagnostic group are presented in Figure 1 and age-adjusted summaries of FA measures are provided in Table 2 (summaries for other diffusion measures are presented in Appendix 1). After adjusting for age, average FA values tended to decrease with disease progression (CS to MCI-DS to DEM). For example, average FA values within the FMinor tract declined from 0.48 (0.47–0.49) to 0.46 (0.43–0.48) to 0.45 (0.42, 0.47) among CS, MCI-DS, and DEM groups, respectively ($P_{trend} = 0.029$, $q_{trend} = 0.099$). Similar patterns were observed in FMajor, L/R ILF, L/R CAB, L/R CCG, and R UNC. Early differences (between CS and MCI-DS) in FA measures were detected within FMajor (−0.04, −0.06 to −0.01; $P = 0.005$, $q = 0.044$), FMinor (−0.02, −0.04 to 0.00; $P = 0.086$, $q = 0.218$), L CCG (−0.03, −0.05 to 0.00; $P = 0.038$, $q = 0.030$), and R CCG (−0.03, −0.05 to 0.00 $P = 0.004$, $q = 0.047$).

Average MD, RD, and AxD diffusion values tended to increase with disease progression (CS to MCI-DS to DEM; Appendix 1). Within FMinor, for example, the average MD values were 0.82 (0.81 to 0.84) in CS, 0.84 (0.80 to 0.88) in MCI-DS, and 0.89 (0.85 to 0.93) in DEM ($P_{trend} = 0.002$, $q_{trend} = 0.028$). Similarly, average FMinor AxD and RD were 1.31 (1.29 to 1.33), 1.31 (1.26 to 1.35), and 1.37 (1.33 to 1.42; $P_{trend} = 0.023$, $q_{trend} = 0.088$) and 0.58 (0.56 to 0.60), 0.61 (0.57 to 0.65), and 0.65 (0.61 to 0.69; $P_{trend} = 0.002$, $q_{trend} = 0.028$). Pairwise differences between CS and MCI were detected only in RD of the FMajor tract (0.05, 0.00 to 0.09; $P = 0.044$, $q = 0.128$).

4.3 | Correlation with predefined clinical measures

Partial Spearman correlations between diffusion measures of the L/R CCG, FMajor, and FMinor, the tracts demonstrating significant

TABLE 3 Partial Spearman correlation (ρ) coefficients between diffusion measure and select neuropsychological instruments, after adjusting for age. Unadjusted *P*-values are reported as all comparisons were predefined

	Diffusion measure	Tract	Left hemisphere		Right hemisphere	
			ρ (95% CI)	*Pvalue*	ρ (95% CI)	*P value*
Total memory score	AxD	CCG	−0.33 (−0.59, 0.00)	0.051	−0.36 (−0.60, −0.05)	0.024
	FA	CCG	0.09 (−0.21, 0.38)	0.554	0.20 (−0.10, 0.46)	0.195
	MD	CCG	−0.36 (−0.62, −0.03)	0.032	−0.38 (−0.62, −0.07)	0.017
	RD	CCG	−0.29 (−0.55, 0.03)	0.072	−0.30 (−0.55, 0.00)	0.051
	AxD	FMajor	−0.14 (−0.42, 0.16)	0.357		
	FA	FMajor	0.26 (−0.02, 0.50)	0.067		
	MD	FMajor	−0.31 (−0.56, 0.00)	0.048		
	RD	FMajor	−0.31 (−0.55, −0.02)	0.039		
	AxD	FMinor	−0.32 (−0.55, −0.04)	0.024		
	FA	FMinor	0.41 (0.10, 0.65)	0.012		
	MD	FMinor	−0.41 (−0.65, −0.09)	0.014		
	RD	FMinor	−0.44 (−0.69, −0.12)	0.010		
Cued Recall	AxD	CCG	−0.30 (−0.57, 0.04)	0.078	−0.27 (−0.54, 0.05)	0.010
	FA	CCG	0.16 (−0.17, 0.46)	0.340	0.25 (−0.05, 0.50)	0.097
	MD	CCG	−0.34 (−0.61, 0.00)	0.051	−0.30 (−0.57, 0.03)	0.077
	RD	CCG	−0.27 (−0.55, 0.06)	0.110	−0.29 (−0.56, 0.04)	0.084
	FA	FMajor	0.32 (0.04, 0.56)	0.029		
	MD	FMajor	−0.36 (−0.60, −0.06)	0.021		
	RD	FMajor	−0.34 (−0.59, −0.04)	0.026		
	FA	FMinor	0.47 (0.19, 0.68)	0.002		
	MD	FMinor	−0.25 (−0.54, 0.09)	0.146		
	RD	FMinor	−0.34 (−0.61, 0.00)	0.048		
Rivermead	RD	FMajor	−0.24 (−0.49, 0.03)	0.083		
	FA	FMinor	0.44 (0.15, 0.66)	0.004		
	RD	FMinor	−0.24 (−0.48, 0.04)	0.088		
TSI	FA	FMinor	0.46 (0.19, 0.68)	0.002		

Abbreviations: AxD, axial diffusivity; ATR, anterior thalamic radiation; CAB, cingulum-angular bundle; CCG, cingulum-cingulate gyrus bundle; CST, corticospinal tract; FA, fractional anisotropy; FDR, false discovery rate; FMajor, forceps major; FMinor, forceps minor; ILF, inferior longitudinal fasciculus; MCI-DS, mild cognitive impairment-Down syndrome; MD, mean diffusivity; RD, radial diffusivity; SLFp, superior longitudinal fasciculus-parietal bundle; SLFt, L/R superior longitudinal fasciculus-temporal bundle; UNC, uncinate fasciculus.

reductions in the MCI-DS group, and predefined neuropsychological tests, after adjusting for age, are provided in Table 3. Most notably, the Total Memory Score was associated with diffusion measures of the CCG tract including MD, AD, and RD. Similar patterns were observed with the FMinor, but not FMajor, tract. The CRT was associated with AD of the CCG tract, with FA, MD, and RD of the FMajor and FA and RD of the FMinor. The Rivermead and TSI were associated with FA of the FMinor.

4.4 | Correlation with predefined regional amyloid (SUVR)

Table 4 summarizes the partial Spearman correlation values between predefined regional amyloid SUVR values and FA values within FMajor, FMinor, and L/R CCG. After adjusting for age, lower FA in the FMinor was significantly associated with higher amyloid burden in the superior frontal, rostral middle frontal, and caudal middle frontal regions (e.g., middle frontal: −0.41, −0.66 to −0.08, $P = 0.016$). Similarly, lower FA in FMajor was associated with increased amyloid in the precuneus (−0.31, −0.57 to 0.00; $P = 0.049$) and inferior parietal regions (−0.34, −0.57 to −0.07; $P = 0.014$) and lower FA in the R/CCG was associated with increased amyloid in the entorhinal (−0.26, −0.50 to 0.02; $P = 0.066$) and inferior parietal cortical regions (−0.28, −0.55 to 0.03; $P = 0.077$).

4.5 | Discrimination using FA diffusion measures

Table 5 summarizes the discriminative ability of FA diffusion measures to distinguish CS from MCI-DS and CS from DEM patients. When

TABLE 4 Partial Spearman correlation coefficients between FA and regional amyloid SUVR after accounting for age. Unadjusted *p*-values are reported since all comparisons were predefined

Tract	Region of interest	ρ (95% CI)	*P-value*
FMinor	Superior frontal	−0.36 (−0.64, 0.01)	0059
	Middle frontal	−0.41 (−0.66, −0.08)	0016
	Caudal middle frontal	−0.37 (−0.65, 0.01)	0058
	Entorhinal cortex	−0.09 (−0.40, 0.25)	0623
FMajor	Precuneus	−0.31 (−0.57, 0.00)	0049
	Superior parietal	−0.16 (−0.44, 0.15)	0303
	Inferior parietal	−0.34 (−0.57, −0.07)	0014
	L lingual	−0.09 (−0.40, 0.24)	0603
	R lingual	−0.10 (−0.38, 0.21)	0545
	Lateral occipital	0.10 (−0.22, 0.40)	0551
R CCG	Entorhinal cortex	−0.26 (−0.50, 0.02)	0066
	Inferior parietal	−0.28 (−0.55, 0.03)	0077
	L parahippocampal	−0.16 (−0.46, 0.17)	0337
	R parahippocampal	0.20 (−0.16, 0.52)	0279
	Precuneus	−0.08 (−0.37, 0.22)	0611
	Superior parietal	−0.13 (−0.43, 0.20)	0454
L CCG	Entorhinal cortex	−0.12 (−0.39, 0.18)	0438
	Inferior parietal	−0.14 (−0.46, 0.20)	0416
	L parahippocampal	0.02 (−0.31, 0.35)	0917
	R parahippocampal	0.16 (−0.19, 0.48)	0370
	Precuneus	0.02 (−0.30, 0.33)	0908
	Superior parietal	0.11 (−0.24, 0.43)	0558

Abbreviations: CCG, cingulum-cingulate gyrus bundle; FA, fractional anisotropy; FMajor, forceps major; FMinor, forceps minor; SUVR, standardized uptake value ratio.

discriminating between MCI-DS and CS, the optimism-corrected area under the ROC curve (oAUC) were: FMajor (0.73, 0.52 to 0.90), FMinor (0.66, 0.41 to 0.84), R/L CCG (0.72, 0.48 to 0.90 and 0.74, 0.48 to 0.88), and R/L ILF (0.68, 0.47 to 0.82 and 0.65, 0.43 to 0.83). The composite FA score included only FMajor and L/CCG (tracts associated with limbic association pathways), which resulted in an oAUC value of 0.76 (0.52 to 0.93). Univariately, nearly all tracts aided in discrimination between DEM and CS patients except CST, ATR, and SLFT. The composite FA score included CCG, ILF SLFP, CAB, and UNC (0.93, 0.80 to 1.00).

5 | DISCUSSION

This study builds on a small body of research focused on MRI-based measures of microstructural integrity in DS and provides support for the importance of white matter abnormalities in the development of dementia in individuals with DS. In MCI-DS, we found evidence of early and specific altered WM integrity of commissural (forceps major) and limbic pathways (cingulum), both late-myelinating fiber bundles. These findings suggest that WM integrity is altered early in the clinical course of AD. Reductions in FA in the FMajor suggest loss of tissue organization; increases in RD suggest the breakdown of neurobiological barriers, such as provided by myelin or cell membranes. The fibers of the FMajor of the corpus callosum arise largely from pyramidal neurons in layers III and V of association cortex; the CCG carries hippocampal projections to the medial temporal lobe. These findings agree with other studies demonstrating early involvement of limbic pathways in preclinical sporadic AD[36-39] as well as in asymptomatic carriers of fully penetrant familial AD.[40] It is notable that early changes in myelin have been found in adults with DS; genes associated with oligodendrocyte differentiation and myelination have been reported to be dysregulated in transgenic mouse models of DS.[2] Similarly, genome-wide transcriptional profiling performed in *post mortem* brains spanning from midfetal development to adulthood found transcriptome alterations in several important pathways including RNA processing, immune responses, axon ensheathment, oligodendrocyte differentiation, and myelination in DS.[2]

Alterations in WM integrity were more widespread in individuals with dementia, including reductions in FA of other tracts and corresponding increases in RD and in AxD; these changes were present in cortico-cortical association pathways (inferior longitudinal fasciculus, superior longitudinal fasciculus), similar to what has been reported in individuals with sporadic AD.[41,42] Interestingly, the cortico-spinal tracts, the ATR and the SLF appeared to be no different between the CS and dementia cohorts. Several studies have suggested that the ATR might already demonstrate altered or less developed structural connectivity in young adults with DS compared with age-matched controls[12,21] and, therefore, may not show additional or progressive changes; this merits further investigation. Early changes in WM integrity of late-myelinating fiber pathways and relative preservation of early myelinating fiber pathways[36,43] supports the retrogenesis model of neurodegeneration in AD progression.[44]

We found that diffusion measures could distinguish among the three groups, defined by their dementia status. FA reductions in the FMajor yielded a high diagnostic accuracy for the clinical diagnosis of MCI and for DEM, supporting the potential development of these measures as clinically relevant biomarkers for dementia in the DS population. The consistency of these findings with what has been reported in MCI,[45,46] in both sporadic AD and autosomal dominantly inherited AD,[47-49] suggests that AD in DS is in fact the same progressive disease process and reinforces the importance of this high-risk population for advancing our understanding of AD more generally.

As hypothesized, we found significant associations between diffusion measures of the CCG, FMajor, and FMinor with memory tests and between more global measures, the Rivermead and TSI and FMinor. Even with a small sample size, these findings support an important role of WM changes in relation to cognitive decline in DS and also suggest that WM microstructural changes may also provide an important and independent biomarker for tracking AD progression.

Significant associations between reduced FA and higher regional amyloid accumulation in associated cortical areas supports suggestions

TABLE 5 Predictive ability of FA diffusion measures to discriminate between CS and MCI-DS and between CS and DEM

	MCI-DS vs CS		DEM vs CS	
	Left hemisphere	Right hemisphere	Left hemisphere	Right hemisphere
Tract	oAUC (95% CI)	oAUC (95% CI)	oAUC (95% CI)	oAUC (95% CI)
FMajor	0.73 (0.52, 0.90)		0.75 (0.48, 0.90)	
FMinor	0.66 (0.41, 0.84)		0.87 (0.73, 0.96)	
CCG	0.74 (0.48, 0.88)	0.72 (0.48, 0.90)	0.68 (0.39, 0.92)	0.79 (0.60, 0.93)
CST	0.51 (0.40, 0.73)	0.52 (0.40, 0.69)	0.53 (0.41, 0.73)	0.55 (0.40, 0.77)
ILF	0.65 (0.43, 0.83)	0.68 (0.47, 0.82)	0.76 (0.57, 0.89)	0.79 (0.55, 0.94)
SLFP	0.54 (0.41, 0.76)	0.51 (0.37, 0.75)	0.72 (0.40, 0.93)	0.71 (0.40, 0.97)
ATR	0.52 (0.39, 0.76)	0.58 (0.40, 0.80)	0.53 (0.37, 0.79)	0.51 (0.38, 0.72)
CAB	0.55 (0.35, 0.76)	0.58 (0.42, 0.76)	0.72 (0.46, 0.90)	0.77 (0.60, 0.89)
SLFT	0.52 (0.39, 0.71)	0.52 (0.38, 0.76)	0.71 (0.39, 0.93)	0.56 (0.32, 0.88)
UNC	0.52 (0.39, 0.72)	0.55 (0.38, 0.82)	0.73 (0.54, 0.87)	0.83 (0.62, 0.95)
Composite	0.76 (0.53, 0.93)[a]		0.93 (0.80, 1.00)[b]	

Optimism corrected area under the ROC curve (oAUC), and their 95% bootstrapped confidence are reported using each tract individually, as well as a composite using a relaxed LASSO approach with 10-fold cross-validation.

[a]FMajor, L CCG.

[b]FMinor, R CCG, R ILF, L/R SLFP, L ATR, R CAB, L/R UNC.

Abbreviations: ATR, anterior thalamic radiation; CAB, cingulum-angular bundle; CCG, cingulum-cingulate gyrus bundle; CST, corticospinal tract; FA, fractional anisotropy; FDR, false discovery rate; FMajor, forceps major; FMinor, forceps minor; ILF, inferior longitudinal fasciculus; MCI-DS, mild cognitive impairment-Down syndrome; MD, mean diffusivity; RD, radial diffusivity; SLFp, superior longitudinal fasciculus-parietal bundle; SLFt, L/R superior longitudinal fasciculus-temporal bundle; UNC, uncinate fasciculus.

that the accumulation of aggregated ß-amyloid 1-42 and the assembly of neurofibrillary tangles are detrimental not only to neurons but also to myelin and myelin-producing oligodendrocytes.[50]

In summary, our work suggests an important pathophysiological link between WM damage, MCI-DS clinical status, and amyloid deposition in DS, prior to the onset of dementia. It supports the use of diffusion weighted imaging as an important and clinically relevant biomarker of early clinical progression of AD in individuals with DS, and may serve as a model for sporadic AD. It will be essential to follow up these observations in a larger longitudinal study.

ACKNOWLEDGMENTS

We are very grateful to the individuals who participated in this study, who so generously contributed their time and energy to this project, and without whom it would not have been possible. We thank the individuals who helped recruit and assess participants for this study including Courtney Jordan, Nusrat Jahan, Eric Doran, Sara Stajcic, Casey Evans, Deborah Pang, Tracey Listwan, Cynthia Kovacs. We thank the individuals who assisted with scanning participants, including Matt Linnehan, Lily Wang, Ana Mun.

REFERENCES

1. Brickman AM, Provenzano FA, Muraskin J, et al. Regional white matter hyperintensity volume, not hippocampal atrophy, predicts incident Alzheimer disease in the community. *Arch Neurol*. 2012;69(12):1621-1627.
2. Olmos-Serrano JL, Kang HJ, Tyler WA, et al. Down syndrome developmental brain transcriptome reveals defective oligodendrocyte differentiation and myelination. *Neuron*. 2016;89(6):1208-1222.
3. Lai F, Williams RS. A prospective study of Alzheimer disease in Down syndrome. *Arch Neurol*. 1989;46(8):849-853.
4. Rumble B, Retallack R, Hilbich C, et al. Amyloid A4 protein and its precursor in Down's syndrome and Alzheimer's disease. *N Engl J Med*. 1989;320(22):1446-1452.
5. Jennings D, Seibyl J, Sabbagh M, et al. Age dependence of brain beta-amyloid deposition in Down syndrome: an [18F]florbetaben PET study. *Neurology*. 2015;84(5):500-507.
6. Handen BL, Cohen AD, Channamalappa U, et al. Imaging brain amyloid in nondemented young adults with Down syndrome using Pittsburgh compound B. *Alzheimers Dement*. 2012;8(6):496-501.
7. Hartley SL, Handen BL, Devenny DA, et al. Cognitive functioning in relation to brain amyloid-beta in healthy adults with Down syndrome. *Brain*. 2014;137(Pt 9):2556-2563.
8. Brun A, Englund E. A white matter disorder in dementia of the Alzheimer type: a pathoanatomical study. *Ann Neurol*. 1986;19(3):253-262.
9. Sjobeck M, Haglund M, Englund E. Decreasing myelin density reflected increasing white matter pathology in Alzheimer's disease–a neuropathological study. *Int J Geriatr Psychiatry*. 2005;20(10):919-926.
10. Gouw AA, Seewann A, Vrenken H, et al. Heterogeneity of white matter hyperintensities in Alzheimer's disease: post-mortem quantitative MRI and neuropathology. *Brain*. 2008;131(Pt 12):3286-3298.
11. Powell D, Caban-Holt A, Jicha G, et al. Frontal white matter integrity in adults with Down syndrome with and without dementia. *Neurobiol Aging*. 2014;35(7):1562-1569.
12. Romano A, Moraschi M, Cornia R, et al. White matter involvement in young non-demented Down's syndrome subjects: a tract-based spatial statistic analysis. *Neuroradiology*. 2018;60(12):1335-1341.
13. Yendiki A, Panneck P, Srinivasan P, et al. Automated probabilistic reconstruction of white-matter pathways in health and disease using an atlas of the underlying anatomy. *Front Neuroinform*. 2011;5:23.
14. Alexander-Bloch AF, Vértes PE, Stidd R, et al. The anatomical distance of functional connections predicts brain network topology in health and schizophrenia. *Cereb Cortex*. 2013;23(1):127-138.

15. Beaulieu C. The basis of anisotropic water diffusion in the nervous system - a technical review. *NMR Biomed*. 2002;15(7-8):435-455.
16. Selemon LD, Goldman-Rakic PS. The reduced neuropil hypothesis: a circuit based model of schizophrenia. *Biol Psychiatry*. 1999;45(1):17-25.
17. Alexander AL, Lee JE, Lazar M, Field AS. Diffusion tensor imaging of the brain. *Neurotherapeutics*. 2007;4(3):316-329.
18. Demirhan A, Nir TM, Zavaliangos-Petropulu A, et al. Feature selection improves the accuracy of classifying Alzheimer disease using diffusion tensor images. *Proc IEEE Int Symp Biomed Imaging*. 2015;2015:126-130.
19. Kantarci K, Avula R, Senjem ML, et al. Dementia with Lewy bodies and Alzheimer disease: neurodegenerative patterns characterized by DTI. *Neurology*. 2010;74(22):1814-1821.
20. Konukoglu E, Coutu J-P, Salat DH, Fischl B, Alzheimer's Disease Neuroimaging Initiative (ADNI). Multivariate statistical analysis of diffusion imaging parameters using partial least squares: Application to white matter variations in Alzheimer's disease. *Neuroimage*. 2016;134:573-586.
21. Fenoll R, Pujol J, Esteba-Castillo S, et al. Anomalous white matter structure and the effect of age in Down Syndrome patients. *J Alzheimers Dis*. 2017;57(1):61-70.
22. Silverman W, Schupf N, Zigman W, et al. Dementia in adults with mental retardation: assessment at a single point in time. *Am J Ment Retard*. 2004;109(2):111-125.
23. Aylward EH, Burt DB, Thorpe LU, Lai F, Dalton A. Diagnosis of dementia in individuals with intellectual disability. *J Intellect Disabil Res*. 1997;41 (Pt 2):152-164.
24. Burt DB, Aylward EH. Test battery for the diagnosis of dementia in individuals with intellectual disability. Working Group for the Establishment of Criteria for the Diagnosis of Dementia in Individuals with Intellectual Disability. *J Intellect Disabil Res*. 2000;44 (Pt 2):175-180.
25. Devenny DA, Zimmerli EJ, Kittler P, Krinsky-McHale SJ. Cued recall in early-stage dementia in adults with Down's syndrome. *J Intellect Disabil Res*. 2002;46(Pt 6):472-483.
26. Wilson BA, Ivani-Chalian R, Besag FM, Bryant T. Adapting the Rivermead Behavioural Memory Test for use with children aged 5 to 10 years. *J Clin Exp Neuropsychol*. 1993;15(4):474-486.
27. Albert M, Cohen C. The Test for Severe Impairment: an instrument for the assessment of patients with severe cognitive dysfunction. *J Am Geriatr Soc*. 1992;40(5):449-453.
28. Haxby JV. Neuropsychological evaluation of adults with Down's syndrome: patterns of selective impairment in non-demented old adults. *J Ment Defic Res*. 1989;33 (Pt 3):193-210.
29. Rosas HD, Salat DH, Lee SY, Zaleta AK, Hevelone N, Hersch SM. Complexity and heterogeneity: what drives the ever-changing brain in Huntington's disease? *Ann N Y Acad Sci*. 2008;1147:196-205.
30. Yendiki A, Reuter M, Wilkens P, Rosas HD, Fischl B. A probabilistic method for unbiased longitudinal tractography with application to Huntington's disease. *Proc Int Soc Mag Res Med*. 2014;2014:4530.
31. Greve DN, Fischl B. Accurate and robust brain image alignment using boundary-based registration. *Neuroimage*. 2009;48(1):63-72.
32. Fischl B. FreeSurfer. *Neuroimage*. 2012;62(2):774-781.
33. Desikan RS, Ségonne F, Fischl B, et al. An automated labeling system for subdividing the human cerebral cortex on MRI scans into gyral based regions of interest. *Neuroimage*. 2006;31(3):968-980.
34. Benjamini Y, Hochberg Y. Controlling the false discovery rate: a practival and powerful approach to multiple testing. *J Roy Statist Soc Ser A*. 1995;57(Series B):289-300.
35. Team RC. A language and environment for statistical computing. R Foundation for STatistical Computing. 2018; Available from: https://www.R-project.org/.
36. Teipel SJ, Bayer W, Alexander GE, et al. Progression of corpus callosum atrophy in Alzheimer disease. *Arch Neurol*. 2002;59(2):243-248.
37. Salat DH, Chen JJ, van der Kouwe AJ, Greve DN, Fischl B, Rosas HD. Hippocampal degeneration is associated with temporal and limbic gray matter/white matter tissue contrast in Alzheimer's disease. *Neuroimage*. 2011;54(3):1795-1802.
38. Lee S-H, Coutu J-P, Wilkens P, Yendiki A, Rosas HD, Salat DH, Alzheimer's disease Neuroimaging Initiative (ADNI). Tract-based analysis of white matter degeneration in Alzheimer's disease. *Neuroscience*. 2015;301:79-89.
39. Zhang X, Sun Y, Li W, et al. Characterization of white matter changes along fibers by automated fiber quantification in the early stages of Alzheimer's disease. *Neuroimage Clin*. 2019;22:101723.
40. Ringman JM, O'Neill J, Geschwind D, et al. Diffusion tensor imaging in preclinical and presymptomatic carriers of familial Alzheimer's disease mutations. *Brain*. 2007;130(Pt 7):1767-1776.
41. Cavedo E, Lista S, Rojkova K, et al. Disrupted white matter structural networks in healthy older adult APOE epsilon4 carriers - An international multicenter DTI study. *Neuroscience*. 2017;357:119-133.
42. Major N, McQuistan MR, Qian F. Changes in Dental Students' Attitudes About Treating Underserved Populations: A Longitudinal Study. *J Dent Educ*. 2016;80(5):517-525.
43. Aeby A, Liu Y, De Tiège X, et al. Maturation of thalamic radiations between 34 and 41 weeks' gestation: a combined voxel-based study and probabilistic tractography with diffusion tensor imaging. *AJNR Am J Neuroradiol*. 2009;30(9):1780-1786.
44. Bartzokis G, Sultzer D, Lu PH, Nuechterlein KH, Mintz J, Cummings JL. Heterogeneous age-related breakdown of white matter structural integrity: implications for cortical "disconnection" in aging and Alzheimer's disease. *Neurobiol Aging*. 2004;25(7):843-851.
45. Di Paola, M., G. Spalletta, C. Caltagirone, In vivo structural neuroanatomy of corpus callosum in Alzheimer's disease and mild cognitive impairment using different MRI techniques: a review. *J Alzheimers Dis*. 2010;20(1):67-95.
46. Di Paola M, Di Iulio F, Cherubini A, et al. When, where, and how the corpus callosum changes in MCI and AD: a multimodal MRI study. *Neurology*. 2010;74(14):1136-1142.
47. Araque Caballero MA, Suárez-Calvet M, Duering M, et al. White matter diffusion alterations precede symptom onset in autosomal dominant Alzheimer's disease. *Brain*. 2018;141(10):3065-3080.
48. Agosta F, Pievani M, Sala S, et al. White matter damage in Alzheimer disease and its relationship to gray matter atrophy. *Radiology*. 2011;258(3):853-863.
49. Chang Y-L, Chen T-F, Shih Y-C, Chiu M-J, Yan S-H, Tseng W-YI. Regional cingulum disruption, not gray matter atrophy, detects cognitive changes in amnestic mild cognitive impairment subtypes. *J Alzheimers Dis*. 2015;44(1):125-138.
50. Bartzokis G, Lu PH, Mintz J. Human brain myelination and amyloid beta deposition in Alzheimer's disease. *Alzheimers Dement*. 2007;3(2):122-125.

How to cite this article: Rosas HD, Hsu E, Mercaldo ND, et al. Alzheimer-related altered white matter microstructural integrity in Down syndrome: A model for sporadic AD? *Alzheimer's Dement*. 2020;12:e12040. https://doi.org/10.1002/dad2.12040

APPENDIX 1: Diffusion measure summaries of selected tracts. Main effect estimates (CS, MCI-DS, and Dementia) correspond to average diffusion values without adjusting for age, while comparison columns (MCI-DS vs CS) correspond to expected diffusion values after adjusting for age. Monotonic trends were assessed using the partial Spearman correlation that accounted for age. Unadjusted *P*-values are presented (*P*) as well as FDR-adjusted *p*-values (*q*) that account for multiple testing of all diffusion measures. Tracts include: forceps major (FMajor), forceps minor (FMinor), L/R corticospinal tract (CST), L/R inferior longitudinal fasciculus (ILF), L/R uncinate fasciculus (UNC), L/R anterior thalamic radiation (ATR), L/R cingulum-cingulate gyrus bundle (CCG), L/R cingulum-angular bundle (CAB), L/R superior longitudinal fasciculus-parietal bundle (SLFp), L/R superior longitudinal fasciculus-temporal bundle (SLFt)

Axial Diffusivity

	Cognitively stable (CS)N = 35	MCI-DSN = 11	DementiaN = 10	P_{trend} (q_{trend})	MCI-DS - CS	MCI-DS - CS; *P* (*q*)
FMajor	1.47 (1.45, 1.49)	1.45 (1.40, 1.49)	1.51 (1.46, 1.56)	0.887 (0.940)	-0.02 (-0.07, 0.02)	0.329 (0.538)
FMinor	1.31 (1.29, 1.33)	1.31 (1.26, 1.35)	1.37 (1.33, 1.42)	0.023 (0.088)	0.00 (-0.04, 0.04)	0.948 (0.973)
L ATR	1.15 (1.14, 1.17)	1.16 (1.12, 1.20)	1.22 (1.18, 1.26)	0.002 (0.028)	0.00 (-0.03, 0.04)	0.873 (0.937)
L CAB	1.19 (1.17, 1.22)	1.19 (1.14, 1.25)	1.24 (1.18, 1.30)	0.323 (0.535)	0.00 (-0.06, 0.06)	0.995 (0.995)
L CCG	1.31 (1.29, 1.33)	1.30 (1.25, 1.34)	1.35 (1.30, 1.39)	0.217 (0.422)	-0.01 (-0.06, 0.03)	0.530 (0.720)
L CST	1.27 (1.25, 1.28)	1.26 (1.22, 1.29)	1.31 (1.27, 1.34)	0.083 (0.214)	-0.01 (-0.04, 0.02)	0.550 (0.720)
L ILF	1.25 (1.23, 1.26)	1.24 (1.20, 1.27)	1.33 (1.30, 1.37)	0.016 (0.074)	-0.01 (-0.05, 0.02)	0.509 (0.718)
L Slfp	1.16 (1.15, 1.18)	1.14 (1.11, 1.17)	1.22 (1.18, 1.25)	0.022 (0.087)	-0.02 (-0.05, 0.01)	0.165 (0.361)
L Slft	1.19 (1.18, 1.21)	1.18 (1.15, 1.21)	1.26 (1.22, 1.29)	0.018 (0.079)	-0.01 (-0.05, 0.02)	0.414 (0.621)
L Unc	1.19 (1.17, 1.21)	1.20 (1.16, 1.23)	1.26 (1.23, 1.30)	0.001 (0.023)	0.01 (-0.03, 0.04)	0.675 (0.824)
R ATR	1.16 (1.14, 1.18)	1.14 (1.11, 1.18)	1.22 (1.18, 1.26)	0.010 (0.059)	-0.01 (-0.05, 0.02)	0.477 (0.680)
R CAB	1.20 (1.17, 1.22)	1.18 (1.13, 1.23)	1.25 (1.20, 1.31)	0.297 (0.590)	-0.02 (-0.07, 0.03)	0.377 (0.584)
R CCG	1.29 (1.27, 1.31)	1.26 (1.22, 1.30)	1.33 (1.28, 1.37)	0.264 (0.463)	-0.03 (-0.07, 0.02)	0.226 (0.428)
R CST	1.27 (1.24, 1.29)	1.25 (1.21, 1.30)	1.30 (1.25, 1.35)	0.220 (0.422)	-0.01 (-0.06, 0.03)	0.542 (0.720)
R ILF	1.26 (1.25, 1.28)	1.24 (1.20, 1.27)	1.32 (1.28, 1.36)	0.141 (0.323)	-0.03 (-0.07, 0.01)	0.131 (0.313)
R Slfp	1.17 (1.15, 1.19)	1.14 (1.11, 1.18)	1.23 (1.19, 1.27)	0.075 (0.200)	-0.03 (-0.06, 0.01)	0.146 (0.327)
R Slft	1.18 (1.15, 1.20)	1.15 (1.11, 1.19)	1.25 (1.21, 1.30)	0.036 (0.115)	-0.03 (-0.07, 0.02)	0.233 (0.431)
R UNC	1.20 (1.18, 1.22)	1.20 (1.16, 1.24)	1.26 (1.22, 1.31)	0.006 (0.048)	0.00 (-0.04, 0.04)	0.936 (0.973)

Mean Diffusivity

	Cognitively stable (CS)N = 35	MCI-DSN = 11	DementiaN = 10	P_{trend} (q_{trend})	MCI-DS - CS	MCI-DS - CS; *P* (*q*)
FMajor	0.83 (0.81, 0.85)	0.85 (0.81, 0.89)	0.87 (0.82, 0.91)	0.074 (0.200)	0.02 (-0.02,0.06)	0.249 (0.448)
FMinor	0.82 (0.81, 0.84)	0.84 (0.80, 0.88)	0.89 (0.85, 0.93)	0.002 (0.028)	0.02 (-0.02,0.05)	0.368 (0.579)
L ATR	0.78 (0.77, 0.80)	0.79 (0.76, 0.81)	0.81 (0.78, 0.84)	0.008 (0.052)	0.00 (-0.03,0.03)	0.953 (0.973)
L CAB	0.85 (0.82, 0.88)	0.86 (0.81, 0.91)	0.91 (0.86, 0.97)	0.082 (0.214)	0.01 (-0.05,0.06)	0.735 (0.868)
L CCG	0.77 (0.75, 0.79)	0.78 (0.75, 0.82)	0.81 (0.78, 0.85)	0.010 (0.059)	0.01 (-0.03,0.04)	0.605 (0.764)
L CST	0.75 (0.74, 0.76)	0.74 (0.72, 0.77)	0.78 (0.75, 0.80)	0.021 (0.086)	0.00 (-0.03,0.02)	0.789 (0.887)
L ILF	0.81 (0.80, 0.83)	0.82 (0.79, 0.84)	0.89 (0.86, 0.92)	0.001 (0.023)	0.00 (-0.03,0.03)	0.857 (0.937)
L Slfp	0.78 (0.77, 0.80)	0.77 (0.75, 0.80)	0.84 (0.81, 0.86)	0.007 (0.048)	-0.01 (-0.04,0.02)	0.454 (0.667)
L Slft	0.78 (0.76, 0.79)	0.77 (0.74, 0.80)	0.83 (0.80, 0.86)	0.011 (0.059)	-0.01 (-0.03,0.02)	0.586 (0.753)
L Unc	0.83 (0.82, 0.84)	0.84 (0.81, 0.87)	0.90 (0.87, 0.93)	0.001 (0.023)	0.01 (-0.01,0.04)	0.391 (0.599)
R ATR	0.79 (0.77, 0.80)	0.78 (0.76, 0.81)	0.82 (0.79, 0.85)	0.014 (0.072)	0.00 (-0.03,0.03)	0.874 (0.937)
R CAB	0.84 (0.82, 0.86)	0.84 (0.81, 0.88)	0.92 (0.88, 0.97)	0.013 (0.069)	0.00 (-0.04,0.04)	0.879 (0.937)
R CCG	0.77 (0.75, 0.79)	0.77 (0.74, 0.81)	0.82 (0.79, 0.86)	0.003 (0.028)	0.00 (-0.03,0.04)	0.837 (0.928)
R CST	0.76 (0.75, 0.78)	0.75 (0.72, 0.79)	0.80 (0.76, 0.83)	0.121 (0.294)	-0.01 (-0.04,0.02)	0.532 (0.720)
R ILF	0.82 (0.81, 0.84)	0.81 (0.78, 0.84)	0.88 (0.85, 0.92)	0.010 (0.059)	-0.01 (-0.04,0.02)	0.596 (0.759)
R Slfp	0.79 (0.77, 0.80)	0.77 (0.74, 0.80)	0.84 (0.81, 0.88)	0.025 (0.088)	-0.02 (-0.05,0.01)	0.198 (0.402)
R Slft	0.78 (0.76, 0.79)	0.76 (0.73, 0.79)	0.83 (0.80, 0.87)	0.024 (0.088)	-0.02 (-0.05,0.01)	0.243 (0.442)
R UNC	0.83 (0.82, 0.84)	0.84 (0.81, 0.86)	0.90 (0.87, 0.93)	0.002 (0.028)	0.01 (-0.02,0.03)	0.707 (0.856)

Radial Diffusivity

	Cognitively stable (CS)N = 35	MCI-DSN = 11	DementiaN = 10	P_{trend} (q_{trend})	MCI-DS - CS	MCI-DS - CS; *P* (*q*)
FMajor	0.51 (0.49, 0.53)	0.56 (0.51, 0.60)	0.55 (0.50, 0.60)	0.027 (0.096)	0.05 (0.00,0.09)	0.044 (0.128)
FMinor	0.58 (0.56, 0.60)	0.61 (0.57, 0.65)	0.65 (0.61, 0.69)	0.002 (0.028)	0.03 (-0.01,0.06)	0.193 (0.402)
L ATR	0.60 (0.59, 0.61)	0.60 (0.57, 0.63)	0.61 (0.58, 0.64)	0.196 (0.402)	0.00 (-0.03,0.03)	0.986 (0.993)
L CAB	0.68 (0.65, 0.71)	0.69 (0.63, 0.76)	0.75 (0.68, 0.82)	0.051 (0.142)	0.01 (-0.05,0.08)	0.659 (0.812)
L CCG	0.50 (0.48, 0.52)	0.52 (0.49, 0.56)	0.55 (0.51, 0.58)	0.007 (0.048)	0.02 (-0.02,0.06)	0.258 (0.458)
L CST	0.49 (0.47, 0.50)	0.49 (0.46, 0.52)	0.51 (0.48, 0.54)	0.024 (0.088)	0.00 (-0.03,0.03)	0.979 (0.993)
L ILF	0.60 (0.58, 0.61)	0.61 (0.58, 0.64)	0.66 (0.63, 0.69)	<0.001 (0.023)	0.01 (-0.02,0.04)	0.539 (0.720)
L Slfp	0.59 (0.58, 0.61)	0.59 (0.56, 0.62)	0.64 (0.61, 0.67)	0.016 (0.074)	0.00 (-0.03,0.02)	0.769 (0.880)
L Slft	0.57 (0.56, 0.58)	0.57 (0.54, 0.59)	0.62 (0.59, 0.65)	0.019 (0.082)	0.00 (-0.03,0.02)	0.770 (0.880)
L Unc	0.65 (0.63, 0.66)	0.66 (0.63, 0.69)	0.72 (0.68, 0.75)	0.004 (0.035)	0.01 (-0.02,0.04)	0.370 (0.579)
R ATR	0.60 (0.59, 0.61)	0.60 (0.58, 0.63)	0.63 (0.60, 0.65)	0.037 (0.115)	0.00 (-0.02,0.03)	0.818 (0.913)
R CAB	0.66 (0.64, 0.68)	0.68 (0.64, 0.72)	0.76 (0.71, 0.80)	0.002 (0.028)	0.02 (-0.03,0.06)	0.464 (0.668)
R CCG	0.51 (0.50, 0.53)	0.53 (0.50, 0.57)	0.57 (0.53, 0.61)	0.001 (0.023)	0.02 (-0.02,0.05)	0.294 (0.509)
R CST	0.51 (0.50, 0.53)	0.51 (0.47, 0.54)	0.54 (0.51, 0.58)	0.133 (0.313)	-0.01 (-0.04,0.02)	0.610 (0.764)
R ILF	0.60 (0.58, 0.61)	0.60 (0.57, 0.63)	0.67 (0.63, 0.70)	0.002 (0.028)	0.00 (-0.03,0.03)	0.873 (0.937)
R Slfp	0.59 (0.58, 0.61)	0.58 (0.55, 0.61)	0.65 (0.62, 0.68)	0.039 (0.117)	-0.02 (-0.05,0.01)	0.304 (0.515)
R Slft	0.58 (0.56, 0.59)	0.57 (0.54, 0.60)	0.62 (0.59, 0.66)	0.148 (0.318)	-0.01 (-0.04,0.02)	0.347 (0.561)
R UNC	0.65 (0.63, 0.66)	0.65 (0.63, 0.68)	0.71 (0.68, 0.74)	0.003 (0.028)	0.01 (-0.02,0.04)	0.545 (0.720)